THE ASTROPHYSICAL JOURNAL, 561:L107–L110, 2001 November 1

X-RAY DETECTION OF PRESUPERNOVA EVOLUTION FOR THE SN 1993J PROGENITOR

STEFAN IMMLER,[1] BERND ASCHENBACH,[2] AND Q. DANIEL WANG[1]
Received 2001 May 24; accepted 2001 September 17; published 2001 October 8

ABSTRACT

We report on the first detection of presupernova evolution in the X-ray regime. The results are based on *ROSAT* observations of SN 1993J ranging from 6 days to 5 years after the outburst. The X-ray observations are used to probe the SN shell interaction with the ambient circumstellar matter (CSM). After exploring various scenarios that might explain the observed X-ray light curve with a $t^{-0.27}$ rate of decline, we present a coherent picture in terms of the interaction of the SN shock front with the CSM deposited by the progenitor's stellar wind. During the observed period, the SN shell reaches a radius of 3×10^{17} cm from the site of the explosion, corresponding to $\sim 10^4$ yr in the progenitor's stellar wind history. Our analysis shows that the mass-loss rate of the progenitor has decreased constantly from $\dot{M} = 4 \times 10^{-4}$ to $4 \times 10^{-5}\ M_\odot\ \mathrm{yr}^{-1}$ (v_w/10 km s^{-1}) during the late stage of the evolution. Assuming a spherically symmetric expansion, the circumstellar matter density profile is found to be significantly flatter ($\rho_{\mathrm{csm}} \propto r^{-1.63}$) than expected for a constant mass-loss rate and constant wind velocity profile (r^{-2}). The observed evolution reflects a decrease in the mass-loss rate, an increase in the wind speed, or a combination of both, indicating that the progenitor likely was making a transition from the red to the blue supergiant phase during the late stage of its evolution.

Subject headings: stars: mass loss — X-rays: individual (SN 1993J) — X-rays: ISM

1. INTRODUCTION

The interaction of a supernova (SN) with circumstellar matter (CSM) produces a fast shock wave in the CSM and a reverse shock wave into the outer SN ejecta. Two characteristic regions of X-ray emission are produced by the interaction: the forward shock wave in the CSM at $T \sim 10^4$ km s^{-1} produces gas with $\sim 10^9$ K, and the reverse shock wave in the SN ejecta $\sim 10^3$ km s^{-1} less than the forward shock produces gas with $T \sim 10^7$ K. The reverse shock is formed where the freely expanding SN ejecta catches up with the CSM shocked by the blast wave. At early times, the reverse shock front is radiative and a dense, cool ($T < 10^4$ K) shell can build up downstream from the radiating region (Chevalier & Fransson 1994). The dense shell can absorb X-rays from the reverse shock region and reprocess them to lower energies.

This scenario was supported by observations of Type IIb SN 1993J with *ROSAT* (Zimmermann et al. 1994, 1996) and with *ASCA* (Kohmura et al. 1994). The early X-ray spectrum at day 6 was hard, with $T \sim 10^{8.5}$ K. At day ~200, a softer component with $T \sim 10^7$ K dominated. The emergence of the softer spectrum could be attributed to the decreased absorption by a cool shell (Fransson, Lundqvist, & Chevalier 1996, hereafter FLC96).

2. THEORETICAL BACKGROUND

The thermal X-ray luminosity L_{X} of the shock-heated plasma is expressed by the product of the emission measure (EM) and the cooling function, $\Lambda(T, Z, \Delta E)$, where T is the plasma temperature, Z represents the elemental abundance distribution, and ΔE is the X-ray energy bandwidth. For spherically symmetric conditions, $\mathrm{EM} = 4\pi \int_{R_0}^{R} n_e^2 r^2\, dr$, where r, the radial coordinate, runs from R_0 to R, the current outer boundary of the shocked matter, which has an electron density n_e. Assuming a constant SN shock wave speed v_s, $R = v_s t$, where t represents the time elapsed since the explosion. If the ambient matter density ρ is dominated by a wind blown by the progenitor star of the SN, the continuity equation requires $\dot{M} = 4\pi r^2 \rho v_w$, with $\dot{M}$ the mass-loss rate and v_w the wind speed. The X-ray luminosity can then be expressed as $L_{\mathrm{X}} = [1/(4\pi)\,\Lambda(T)]\,(\dot{M}/v_w)^2 (v_s t)^{-1}$. We can hence use the X-ray luminosity to measure the ratio $\dot{M}/v_w$ of the progenitor star.

Each X-ray measurement at t is related to the corresponding distance from the site of the explosion. This site had been reached by the wind at a time depending on v_w or the age of the wind $t_w = t v_s / v_w$. Usually, $v_s \gg v_w$ so that with a t of only a few years we can look back in time quite an appreciably large time span in the evolution of the progenitor's wind. Assuming that v_w did not change over t_w, we can even directly measure the mass-loss rate back in time. Whether v_w = constant is a reasonable assumption will be discussed below. Integration of the mass-loss rate along the path of the expanding shell gives the mean density inside a sphere of radius r. For a constant wind velocity v_w and mass-loss rate $\dot{M}$, a $\rho_{\mathrm{csm}} = \rho_0 (r/r_0)^{-s}$ profile with $s = 2$ is expected.

After the expanding shell becomes optically thin, it is expected that emission from the SN ejecta itself, heated by the reverse shock, dominates the X-ray output of the interaction regions owing to its higher emission measure and higher density. For a uniformly expanding ejecta, the density structure is a function of its expansion velocity, v, and the time after the explosion, t: $\rho_{\mathrm{sn}} = \rho_0 (t/t_0)^{-3} (v/v_0)^{-n}$, with ρ_0 the ejecta density at time t_0 and v_0 the velocity (FLC96). For a red supergiant progenitor, the power law is rather steep with index $n \sim 20$ (Shigeyama et al. 1994; Baron, Hauschildt, & Branch 1994; Suzuki & Nomoto 1995; FLC96). For constant n, the radius of the discontinuity surface between the forward and reverse shock evolves in time t with $R_c \propto t^m$, where $m = (n-3)/(n-s)$ is the deceleration parameter.

3. X-RAY OBSERVATIONS AND ANALYSIS

SN 1993J in M81 was observed in five individual pointings with the Position Sensitive Proportional Counter (PSPC) and in 10 individual pointings with the High Resolution Imager

[1] Astronomy Department, University of Massachusetts, Amherst, MA 01003.
[2] Max-Planck-Institut für Extraterrestrische Physik, Postfach 1312, 85741 Garching, Germany.

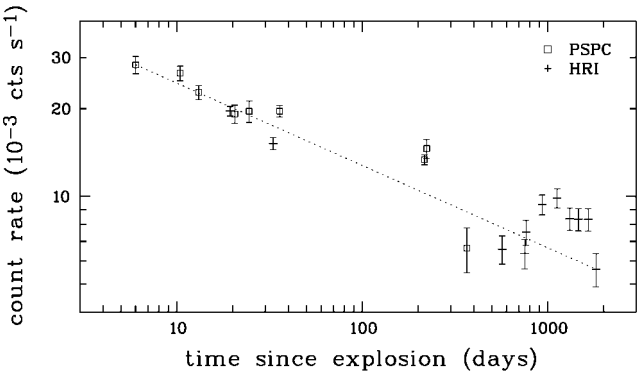

FIG. 1.—*ROSAT* (0.5–2 keV band) X-ray light curve of SN 1993J. Open squares mark PSPC data, HRI data are indicated by crosses. Error bars are 1 σ statistical errors. Dotted line illustrates a $t^{-0.27}$ rate of decline.

(HRI) on board *ROSAT* (Trümper 1983). Total integration times with the PSPC and HRI instruments are 52.2 and 140.3 ks, respectively. Assuming an initial explosion on 1993 March 28 (Ripero 1993), the observations cover a period of 6–1821 days after the outburst. A detailed description of the data calibration and analysis can be found in Immler & Wang (2001).

In order to investigate the rate of decline for SN 1993J, we constructed a combined PSPC+HRI light curve, which is presented in Figure 1. HRI data were binned into 11 continuous observation blocks with 5–20 ks exposure time each to obtain satisfactory counting statistics. PSPC data were binned into nine intervals with 2–18 ks integration time each. The time-dependent background was determined by normalizing the total background map of the HRI and PSPC images according to the total source-removed count rate in each exposure interval. Background-subtracted source counts were extracted within the 90% radii around the fixed position of SN 1993J. In order to reduce background due to UV emission and cosmic rays, only HRI pulse intensity channels 2–10 were used.

An effective 0.5–2 keV band cooling function of $\Lambda = 3 \times 10^{-23}$ ergs cm^{+3} s^{-1} is adopted for an assumed optically thin thermal plasma with a temperature of 10^7 K (Raymond, Cox, & Smith 1976). The equivalent count rate–to–(unabsorbed) flux conversion factor is 4×10^{-11}(ergs cm^{-2} s^{-1})/(counts s^{-1}) for a Galactic column density of $N_{\rm H} = 4 \times 10^{20}$ cm^{-2} (Dickey & Lockman 1990). *ROSAT* HRI and PSPC count rates were converted using a factor of 3, appropriate for the assumed source spectrum (see Immler & Wang 2001). HRI count rate–to–flux conversion factors as a function of spectral model parameters are given in Figure 5 in Wang, Immler, & Pietsch (1999). The uncertainty of the HRI (PSPC) conversion factors for optically thin thermal spectra with temperature in the range 10^7–$10^{8.5}$ K (see § 1) is 22% (19%). An increase in absorbing column from 10^{20} to 10^{21} cm^{-2} increases the unabsorbed source fluxes by ~15%. Assuming an 0.86 keV thermal Bremsstrahlung spectrum (corresponding to a temperature of 10^7 K) instead of a Raymond & Smith thermal plasma reduces the HRI (PSPC) conversion factor by 4% (1%).

4. DISCUSSION

4.1. *X-Ray Emission from the Shock-heated Stellar Wind*

We will first discuss the observed X-ray light curve in the context of the shock-heated stellar wind model and explore other scenarios later. In order to derive the stellar wind age prior to the outburst, an initial wind velocity of $v_w = 10$ km s^{-1} and

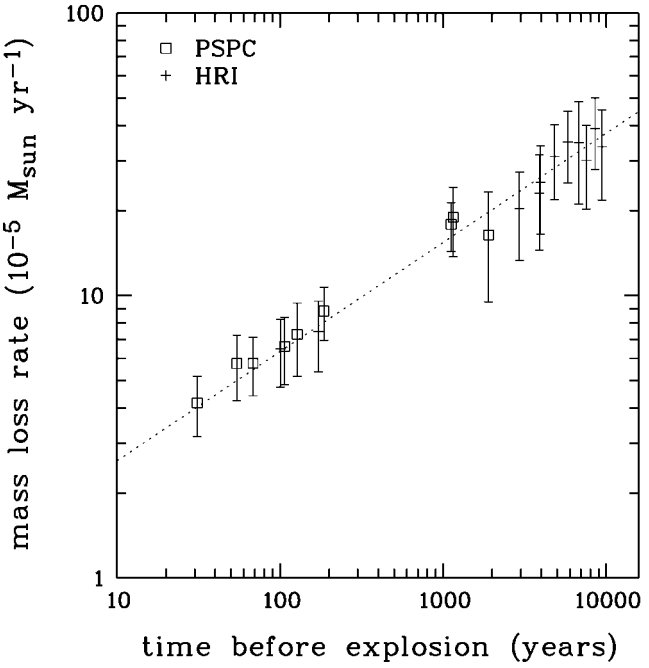

FIG. 2.—Mass-loss rate history of the SN 1993J progenitor. PSPC data are marked by open squares; HRI data are indicated by crosses.

shock front velocity of $v_s = 19{,}900$ km s^{-1} are assumed (Bartel et al. 1994). The choice for the stellar wind speed is justified by the fact that SN 1993J is a Type IIb SN with a massive (~15 $M_\odot$ ZAMS) red supergiant progenitor (e.g., Podsiadlowski et al. 1993). Typical outflow velocities for these progenitors are in the range 3 km s^{-1} $\lesssim v_w \lesssim$ 30 km s^{-1}, peaking at ~10–15 km s^{-1} (e.g., Barnbaum, Kastner, & Zuckermann 1991).

Since the shock front catches up with the wind deposited by the progenitor with a speed of up to ~2000 times larger, the interaction front can be used to probe the stellar wind history over a period of ~10^4 yr. Our X-ray observations can hence be used as a "time machine" to directly measure the CSM density during the last stages of the stellar evolution.

Figure 2 illustrates the change in mass-loss rate as a function of the stellar wind age. It can be seen that the mass-loss rate constantly declined from $\dot{M} = 4 \times 10^{-4}$ to 4×10^{-5} $M_\odot$ yr^{-1} (v_w/10 km s^{-1}) just prior to the explosion. Integration of the mass lost by the progenitor along the shock front gives the CSM density at the given interaction radius from the SN site. The CSM density distribution is illustrated in Figure 3. It is found that the CSM density profile is best described by a power law $\rho_{\rm csm} \propto r^{-s}$ with index $s = 1.63 \pm 0.02$, assuming a spherically symmetric expansion. This is significantly flatter than expected for a constant mass-loss rate and constant wind velocity profile (r^{-2}). The results confirm previous evidence for a rather flat CSM density profile during the first year ($s \sim 1.5$: van Dyk et al. 1994; $1.5 \gtrsim s \gtrsim 1.7$: FLC96; $s = 1.66^{+0.12}_{-0.25}$: Marcaide et al. 1997).

The observed change in the pre-SN history could be due to variations in one of the following parameters:

1. Variations in velocity and/or temperature of the shocked CSM may have caused changes in the X-ray output of the shocked region. This model was proposed to explain the radio light curve of SN 1993J (Fransson & Björnsson 1998). In fact, evidence for a $\lesssim$20% decrease in the expansion velocity over the first ~4 yr was reported (Marcaide et al. 1997; Bartel et al. 2000). This change in shock expansion velocity, however,

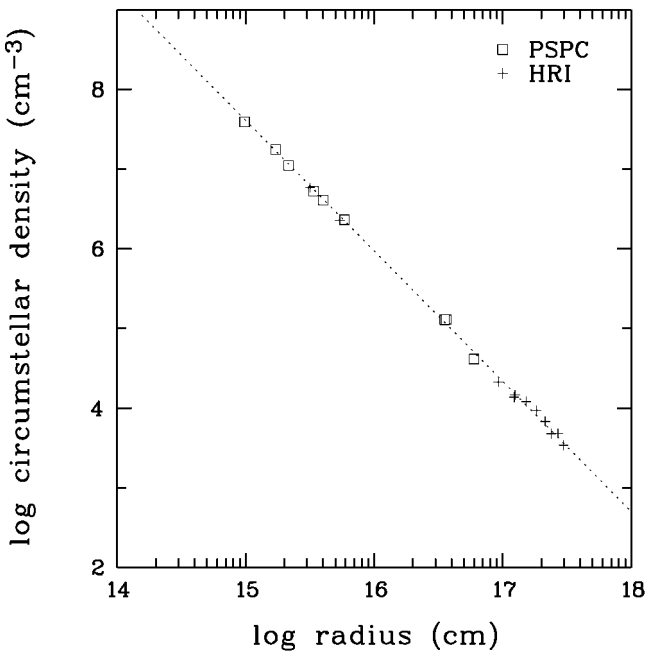

FIG. 3.—Circumstellar density profile as a function of SN shell expansion radius. The dotted line gives the best-fit CSM profile of $\rho_{\rm csm} \propto r^{-1.63}$ to the PSPC (*open squares*) and HRI (*crosses*) data points.

would only lead to a less than 10% increase in the mass-loss rate and cannot account for the observed order-of-magnitude change. Also, as the *ROSAT* soft X-ray band cooling function for optically thin thermal plasma emission is not very sensitive to the plasma temperature [$\Lambda(T) \propto T^{0.5}$; e.g., Raymond, Cox, & Smith 1976], a change in temperature from 10^7 K to a few times 10^{11} K would be required to explain the observed change in the mass-loss rate history. Such drastic temperature variations have been neither observed for SNe nor put forward by models describing the CSM interaction. Therefore, variations in either the shock expansion velocity or the temperature accounting for the inferred evolution can be ruled out.

2. A different scenario would be a nonspherically symmetric geometry caused by a binary evolution of the progenitor. Observational evidence that the progenitor of SN 1993J was a stripped supergiant in a binary system has been presented based on the visual light curve, which cannot be described by a single massive star alone (e.g., Podsiadlowski et al. 1993). In addition, "double-horned" emission-line profiles indicate the presence of a flattened or disklike expanding shell (Matheson et al. 2000a, 2000b). The X-ray light curve also shows some significant deviations from the long-term $t^{-0.27}$ behavior (see Fig. 1). Such deviations have also been observed for SN 1979C in the radio regime (Montes et al. 2000) and were discussed in the context of a self-colliding binary stellar wind model leading to the formation of a multiple shell–like CSM profile (Schwarz & Pringle 1996). X-ray observations of SN 1979C, however, were not suited to address these questions (Immler, Pietsch, & Aschenbach 1998; Kaaret 2001). Similarly, a binary model for SN 1993J cannot be challenged by the *ROSAT* data alone, and no information about the long-term radio light curve of SN 1993J is available.

3. Alternatively, the observed evolution is caused by changes in the wind parameters. The X-ray light curve implies that $\rho_{\rm csm} \propto r^{-s}$ with $s = 1.63$, or using the continuity equation, $\dot{M}/v_w \propto r^{2-s} \propto r^{0.37} \propto t_w^{0.37}$. The ratio $\dot{M}/v_w$ therefore decreases with time approaching the date of the explosion, indicating a decrease in the mass-loss rate, an increase in the wind speed, or a combination of both. It is interesting to compare typical wind parameters for red and blue supergiants, which are on the same evolutionary track for massive ($\gtrsim 15\ M_\odot$ ZAMS) stars (e.g., Salasnich, Bressan, & Chioso 1999). Whereas the mass-loss rate at $t_w \sim 10^4$ yr [$\dot{M} = 4 \times 10^{-4}\ M_\odot$ yr^{-1} (v_w/10 km s^{-1})] is typical for a red supergiant (e.g., $\dot{M} = 3 \times 10^{-4}\ M_\odot$ yr^{-1} for HD 179821; Jura, Velusamy, & Werner 2001; Chin & Stothers 1990; Schaller et al. 1992), the observed change in ratio $\dot{M}/v_w$ by an order of magnitude at $t_w \sim 30$ yr could indicate a transition between the red and blue supergiant phase due to an increase in effective temperature of the star. Blue supergiants are known to have significantly lower mass-loss rates and higher wind velocities ($\dot{M} \sim 10^{-6}\ M_\odot$ yr^{-1}, $v_w \sim 500$–1000 km s^{-1}; e.g., Kudritzki et al. 1999). This scenario for the evolution of the SN 1993J progenitor would have some interesting similarities with that of SN 1987A, whose progenitor completely entered the blue supergiant phase after significant mass transfer to a companion (Podsiadlowski et al. 1993).

Whereas our X-ray data alone cannot give information on whether $\dot{M}$ or v_w have effectively changed during the late stage of the progenitor's evolution, there is a clear difference between these possibilities regarding the kinetical energy of the stellar wind: using $\rho_{\rm csm} \propto r^{-1.63}$, the kinetical wind energy decreased by a factor of 13 for a changing $\dot{M}$ during the observed $\Delta t_w \sim 10^4$ yr. In the scenario of a changing v_w only, an increase in kinetical wind energy by a factor of $10^{2.2}$ is expected. Future stellar evolutionary models might give answers as to which of the two possibilities is more likely.

4.2. *X-Ray Emission from the Shock-heated SN Ejecta*

Let us explore the scenario that the X-ray emission is dominated by the ejecta, heated by the reverse shock. A necessary condition for the ejecta accounting for the observed X-ray emission is that the absorption by the postshock gas is low. In this model, an ejecta density structure of $\rho_{\rm sn} = \rho_0 (t/t_0)^{-3} (v/v_0)^{-n}$ is expected (FLC96). The total X-ray output of both the reverse-shock–heated ejecta and the shocked stellar wind in the forward shock is then given by $L_{\rm X} \propto (\dot{M}/v_w)^2 (t/t_0)^{3-2s}$ in the case where n is large. In fact, using our inferred X-ray rate of decline of $L_{\rm X} \propto t^{-0.27}$ is entirely consistent with the above $L_{\rm X} \propto t^{3-2s} \propto t^{-0.24}$ for $s = 1.63$. The assumption that n must be large is hence confirmed by our data and has also been concluded from radio and optical observations of SN 1993J ($n \sim$ 20–30; Shigeyama et al. 1994; Baron et al. 1994; Suzuki & Nomoto 1995; FLC96). It is important to note that if the density gradient for the ejecta is large, X-rays from the reverse shock must be heavily absorbed. Whereas variations in temperature of the ejecta can be ruled out to explain the observed X-ray light curve (see § 4.1), a change in absorption from initially 10^{22} cm^{-2} to the Galactic column of 4×10^{20} cm^{-2} could account for the observed decrease in source flux (see Fig. 5 in Wang et al. 1999). The signature of high absorption, however, is absent in all *ROSAT* PSPC spectra of SN 1993J, which are consistent with the Galactic foreground absorption [$N_{\rm H} = (5.3 \pm 1.7) \times 10^{20}$ cm^{-2}; Zimmermann et al. 1994, 1996]. The most likely scenario is hence that the emission from the reverse shock is completely absorbed and that the observed soft X-rays are only due to the shocked CSM of the progenitor wind.

Based on the modeling of the early X-ray light curve of SN 1993J, Fransson, Lundqvist, & Chevalier (FLC96) concluded

that the X-ray emission during the first months originates from the interaction of the SN shock with the CSM. As the reverse shock begins to penetrate the cool shell it is expected to contribute an increasing fraction to the total X-ray output. This predicted rise of the *ROSAT* band X-ray flux after ~100 days (as illustrated in Figs. 8 and 10 in FLC96) due to the emerging ejecta is not observed with *ROSAT*. Instead, the overall long-term X-ray light curve (Fig. 1) is declining with a power law close to the initial measurements, which were consistently explained as a result of the interaction of the SN shell with the ambient CSM.

5. CONCLUSIONS

We present the first detection of a pre-SN evolution in X-ray, based on long-term monitoring of SN 1993J with *ROSAT* over a period of 5 yr. The data are fully consistent with a description in the context of the SN shock interacting with the CSM blown off by the progenitor's stellar wind. From the X-ray rate of decline, $L_X \propto t^{-0.27}$, we infer a CSM profile $\rho_{csm} \propto r^{-1.63}$, which is significantly flatter than expected for a constant mass-loss rate and constant wind velocity profile (r^{-2}). The observations cover an epoch of $\sim 10^4$ yr in the progenitor's stellar wind history. During this period, the mass-loss rate of the progenitor has decreased constantly from $\dot{M} = 4 \times 10^{-4}$ to $4 \times 10^{-5}\ M_\odot\ \mathrm{yr}^{-1}$ (v_w/10 km s^{-1}) just prior to the explosion. The most likely explanation for this pre-SN evolution is either an increase in wind speed, a decrease in mass-loss rate or a combination of both, indicative that the progenitor star was undergoing a transition from the red to the blue supergiant phase. The data demonstrate the scientific potential of long-term X-ray monitoring of SNe as an important diagnostical tool to probe the CSM interaction and the evolution of SN progenitors.

This research made use of various online services and databases, e.g., ADS, HEASARC, NED, and the *ROSAT* data archive at MPE. The project is supported by NASA under grants NAG 5-8999 and NAG 5-9429.

REFERENCES

Barnbaum, C., Kastner, J. H., & Zuckermann, B. 1991, AJ, 102, 289
Baron, E., Hauschildt, P. H., & Branch, D. 1994, ApJ, 426, 334
Bartel, N., et al. 1994, Nature, 368, 610
———. 2000, Science, 287, 112
Chevalier, R. A., & Fransson, C. 1994, ApJ, 420, 268
Chin, C.-W., & Stothers, R. B. 1990, ApJS, 73, 821
Dickey, J. M., & Lockman, F. J. 1990, ARA&A, 28, 215
Fransson, C., & Björnsson, C.-I. 1998, ApJ, 509, 861
Fransson, C., Lundqvist, P., & Chevalier, R. A. 1996, ApJ, 461, 993 (FLC96)
Immler, S., Pietsch, W., & Aschenbach, B. 1998, A&A, 331, 601
Immler, S., & Wang, Q. D. 2001, ApJ, 554, 202
Jura, M., Velusamy, T., & Werner, M. W. 2001, ApJ, 556, 408
Kaaret, P. 2001, ApJ, in press (astro-ph/0106568)
Kohmura, Y., et al. 1994, PASJ, 46, L157
Kudritzki, R. P., et al. 1999, A&A, 350, 970
Marcaide, J. M., et al. 1997, ApJ, 486, L31
Matheson, T., et al. 2000a, AJ, 120, 1487
———. 2000b, AJ, 120, 1499
Montes, M. J., et al. 2000, ApJ, 532, 1124
Podsiadlowski, P., Hsu, J. J. L., Joss, P. C., & Ross, R. R. 1992, Nature, 364, 509
Raymond, J. C., Cox, D. P., & Smith, B. W. 1976, ApJ, 204, 290
Ripero, J. 1993, IAU Circ. 5731
Salasnich, B., Bressan, A., & Chioso, C. 1999, A&A, 342, 131
Schaller, G., Schaerer, D., Meynet, G., & Maeder, A. 1992, A&AS, 96, 269
Schwarz, D. H., & Pringle, J. E. 1996, MNRAS, 282, 1018
Shigeyama, T., et al. 1994, ApJ, 420, 341
Suzuki, T., & Nomoto, K. 1995, ApJ, 455, 658
Trümper, J. 1983, Adv. Space Res., 2, 241
van Dyk, S. D., Weiler, K., Sramek, R. A., Rupen, M. P., & Panagia, N. 1994, ApJ, 432, L115
Wang, Q. D., Immler, S., & Pietsch, W. 1999, ApJ, 523, 121
Zimmermann, H. U., Lewin, W. H. G., & Aschenbach, B. 1996, in Proc. Röntgenstrahlung from the Universe, ed. H. U. Zimmerman, J. Trümper, & H. Yorke (MPE Rep. 263; Garching: MPE), 298
Zimmermann, H. U., et al. 1994, Nature, 367, 621